Molecular-dynamics studies of systems of confined dumbbell molecules

Wen-Jong Ma
Department of Physics, The Pennsylvania State University, University Park, Pennsylvania 16802 and Department of Physics, National Central University, Chung-Li 32054, Taiwan, Republic of China

Lakshmanan K. Iyer and Saraswathi Vishveshwara
Molecular Biophysics Unit, Indian Institute of Science, Bangalore 560012, India

Joel Koplik
Benjamin Levich Institute and Department of Physics, City College of New York, New York, New York 10031

Jayanth R. Banavar
Department of Physics, The Pennsylvania State University, University Park, Pennsylvania 16802
(Received 3 December 1993; revised manuscript received 2 June 1994)

We present the results of molecular-dynamics simulations of systems of dumbbell molecules confined by parallel molecular walls. We have carried out systematic studies of three cases: freezing, steady flows, and stick-slip friction. We find that the molecular orientational degrees of freedom cause the surface layers to deviate from a planar configuration. Nevertheless, steady flows, in a channel as narrow as 15 molecular sizes, display continuum behavior. A range of mechanisms in the dynamics of the freezing of a confined fluid is found, as a function of the wall-fluid interactions and the bond length of the dumbbell molecules. The simple order-disorder transition associated with stick-slip motion in the presence of a layer of monoatomic lubricant molecules is supplanted by more complex behavior due to rotational degrees of freedom of the diatomic molecules.

PACS number(s): 68.45.−v, 46.30.Pa, 47.60.+i

I. INTRODUCTION

An understanding of the novel properties of confined fluids is fundamentally important in the development of a complete theory of liquids and vital in applications in diverse areas such as interfacial adhesion, lubrication, rheology, and tribology. As an increasing amount of experimental data becomes available [1,2], there is a need for direct simulation of the molecular dynamics of confined dense liquids in order to interpret and understand the, often, indirect measurements. Molecular dynamics (MD) simulations are a powerful tool for getting information at small length scales and short time scales, especially when such information is not directly available from experiments. In spite of the limitations of length and time scales, recent work [3] and indeed our present study shows that continuum properties are obtained in system sizes, as small as ten molecules across in each of the three directions.

Recently, several experimental studies of the freezing of geometrically confined molecular fluids [1,4] have shown interesting results. The depressed freezing point of oxygen in porous glass had been explained in terms of the geometrical effect arising from the thermodynamically less favored wall-solid interface in the frozen state [1]. On the other hand, detailed structural studies of oxygen, deuterium, and nitrogen in sol gel and vycor glasses suggest other possible complications in the supercooled liquid phase [4]. In our first attempt to investigate the subject using MD simulations [4,5], we found that a novel wall-induced layer-by-layer mechanism of freezing governs the nucleation of the supercooled liquid, which is initiated by the partially ordered surface layers near the wall surfaces. Similar ordering-dictated phenomena have also been found in two other contexts. An MD study [6] of boundary layers in confined flows shows that an increase in the ordering of the surface layers may drive a steady flow with a slip boundary condition towards one that locks at the boundary. Second, in MD studies of the friction between two solid plates [7], the destruction of the ordering of a thin atomic lubricant layer during slipping has been taken as evidence of a thermodynamic instability being the source of the experimentally observed stick-slip mechanism [2]. Subsequent research in this latter case has revealed that the mechanism may involve a variety of state changes other than the simple order-disorder transition when the confined fluid molecules have complex structures [8,9]. Nevertheless, the involvement of phase transitions seems to be robust, as the viscous response to the shear in both simulations and experiments display universal behavior akin to the glass transition [8]. While the fluid molecules used in these simulations are either monoatomic with isotropic interaction potentials, or linear chains imitating polymer molecules, it seems worthwhile to carry out a systematic study of the effects due to the deviation of spherical symmetry and the presence of extra molecular degrees of freedom in the simplest possible case. To achieve this goal, we consider confined systems of simple diatomic molecules. Our dumbbell molecules have a rigid constraint of a fixed

bond length between the two atoms. This seems especially relevant for the freezing studies, since the liquids used in the experimental studies were of this type.

In this study, we have carried out MD simulations of fluids of simple linear molecules between two parallel atomic plates. Our focus has been on monitoring the behavior of the surface layers in two situations: flowing liquids and supercooled liquids, both confined in channels 10–15 molecular sizes wide. The effects of the surface layers on the dynamical behavior of the rest of the system are elucidated. We also present simulations of the stick-slip motion of two atomic plates separated by a lubricant layer in two cases: in one the lubricant consists of a monolayer of spherical molecules, in the second, dumbbell molecules. The former is a test case and the latter serves to underscore the changes caused by the additional degrees of freedom of the confined fluid. In the presence of steady flows, we compare the velocity and the stress tensor profiles to the solutions of the hydrodynamic equations, in principle valid for length and time scales much larger than the molecular states. While both no-slip and slip behaviors are found, depending on the wall-fluid interaction, the behavior of flows in channels as small as 15 molecular sizes is found to be described by continuum hydrodynamics. Even though the amorphous surface layers do not make the fluid-flow non-Newtonian, they suppress the novel wall-induced mechanism of freezing observed in fluids containing spherical molecules. Indeed, we were able to observe the return of the wall nucleation mechanisms on reducing the bond length of the molecules. We monitored the molecular motion by calculating the time correlation functions of the dynamical variables. We found that while the walls strongly affect the relaxational dynamics of the molecular motions in the surface layers, the effects do not significantly extend beyond the region. Finally, the simple phenomenon of ordering and disordering of the lubricant associated with stick and slip is supplanted by more complex behavior in the presence of dumbbell molecules.

In the next section, we present a description of the systems studied. The results of the simulations are in Sec. III. We analyze the structural information of the surface layers obtained in several static cases in Sec. III A. Sections III B–III D include the detailed results of the dynamics of freezing, steady flows, and stick-slip friction. In the last section, we present a summary.

II. MODEL

In most of our simulations, the length of the rigid bond between the two equal-mass interaction sites on a dumbbell molecule was chosen to be $l=0.329\sigma$, where σ is the length parameter of the Lennard-Jones (LJ) atomic interaction potential

$$V_{\mathrm{LJ}}(r)=4\epsilon\{(r/\sigma)^{-12}-(r/\sigma)^{-6}\} . \quad (1)$$

This bond-to-interaction-length ratio is appropriate for a nitrogen molecule [10]. The weak orientational correlation of nitrogen molecules enables us to study the role played by the walls in inducing orientational ordering. Meanwhile, the ratio of the critical temperature to the triple point temperature of nitrogen is approximately 2, which is very close to that of an atomic fluid, e.g., Argon, interacting via the same interaction potential [Eq. (1)] [11]. This allows us to study the dumbbell fluids at a similar relative position in the phase diagram as in previous simulations of monoatomic fluids. We considered three systems. Systems A and B contain 1372 dumbbell molecules each, confined by two pieces of flat parallel walls with separations 16.82σ and 12.85σ, respectively. The densities of the two systems ($\rho^*\equiv\rho\sigma^{-3}=0.63$ for A and $\rho^*=0.836$ for B), fall in the ranges ideal for the studies of flows (system A) and freezing (system B). We have also prepared system C, where a single layer of 112 dumbbell molecules is confined in the same geometry. The gap for system C is in the range $(1.3–2.2)\sigma$, depending on the external load and the thermodynamic conditions. In all systems, periodic boundary conditions are applied in the transverse directions. A few other special systems that have also been considered in our studies are listed in Table I, which will be described when the simulation results are presented.

The walls consist of Lennard-Jones atoms, each with mass 2.5 times that of a dumbbell molecule, in an fcc structure incorporating geometrical corrugations. The relative positions in the transverse (x and y) directions of the two walls were chosen neither in registry nor perfectly out of registry, to avoid possible artifacts. Similar walls had been used in our previous MD studies [5] of supercooled spherical molecule fluids. In all cases, the faces in contact with the fluid are the (100) surfaces with an area $(11.30\sigma)^2$. (We use σ and ϵ to denote the parameters σ_{ff} and ϵ_{ff}, respectively, of the interactions between the atoms of the fluid molecules.) The walls maintain their stability via the interaction potential (1) with a relatively deep potential well of $\epsilon_{ww}=64.1\epsilon$ and $\sigma_{ww}=0.81\sigma$, among its atoms. They are used as thermal baths to control the temperature of the fluids. The thermal velocities of those wall atoms not in direct contact with the fluids, were rescaled so as to give distributions in accord with the desired temperature in all our simulations, unless stated otherwise. Note that the lattice constant ($\sim 1.26\sigma$) of the walls, the interaction parameters σ_{ww} and σ_{ff}, and the bond length l were chose in an incommensurate way to ensure the generality of the results. Gear's fifth order predictor-corrector algorithm [12] was used to integrate the translational dynamic equations and up to the fourth order for the angular momenta and the orientation quaternions, which we used as dynamic variables for the rotational degrees of freedom. The integration time steps in our simulations are $0.001\tau[\tau\equiv(M\sigma^2/2\epsilon)^{1/2}$, M is the mass of the molecule] for systems A and C, and $0.001\,195\,2\tau$ for system B. We chose the cutoff of the interaction potential as 2.3σ in all cases.

III. SIMULATIONS

A. Surface layers

In a diatomic molecule fluid system confined in a planar channel, two effects are important in determining the

properties of the surface layers [5,6]. The first is the tendency of ordering, dominated by the interaction between the walls and the fluid. The second is the effect of close-packing. At a density much lower than the vapor saturation density, the adsorbed surface molecules form various ordered or partially-ordered states with molecules oriented parallel to the basal planes [13]. At a higher density, the interactions with the fellow dumbbell molecules would make these parallel-oriented configurations less favored for the surface molecules. If the density of the system is higher than the triple point density, the effect of closed packing is important. From a purely geometric consideration, a low-temperature-high-density state of the system would have a layered structure, with the surface molecules oriented parallel to the walls if the wall surfaces were smoothly planar. In most cases, however, the orientational degrees of freedom of molecules and the corrugation in molecular scales on wall surfaces, bring in more complications in determining the equilibrium configurations. We have carried out detailed examinations of the surface layers in our model systems by tuning various control parameters, such as temperature, density, bond length, and the strength of the interaction between the walls and the fluid. Our results indicate that the surface layers are characterized by quite different properties from those in the confined spherical molecule systems. As mentioned in Sec. II, we chose the lattice parameter of the walls to be comparable, but incommensurate with the size and bond length of the dumbbell molecules, to ensure the generality of the results.

In previous MD studies of the dynamical behavior of spherical molecule fluids confined in a channel [5,6,14], it was found that the planar geometry of the walls caused ordering in the fluid. The sharp oscillations of the density profile near a wall displayed perpendicular ordering in that region. With an attractive interaction between the molecules of the walls and of the fluid, the well-defined surface layer near a wall is characterized by in-plane ordering. The property is found to be related to the size of the boundary layers in steady channel flows [6]. The same ordering is responsible for the induced layer-by-layer freezing mechanism occurring in a quenched dense liquid [5]. In the presence of a lubricant layer in the narrow gap between two sliding plates, the destruction of the in-plane ordering explains the origin of the stick-to-slip mechanism [7]. In the systems of confined dumbbell molecule fluids, the properties of the surface layers are affected by the molecular asymmetry and orientational degrees of freedom. While the governing planar geometry leads to layering (Fig. 1), the molecules in a surface layer have neither orientational ordering nor strong translational correlations. A detailed examination reveals that the orientations of the molecules in the layer reflect very little the preference of direction imposed by the walls, as a result of two incompatible lengths, determined by the periodicity of the wall atoms and the bond length of the dumbbell molecules, respectively. With stronger wall-fluid interaction, higher density or lower temperature, an increased number of molecules on the surface layers tend to lie parallel to the walls. The effect is, however, so insignificant that, as far as the molecular orientation is concerned, the layer is more three-dimensional than planar.

Figure 2 shows the histograms of the distribution $(d^2N/d\Omega dz)$ of the confined static liquid of system B, where $d\Omega \equiv \sin(\theta)d\theta$, θ is the angle between the axis of a molecule and the z axis—the plane of the walls is defined to be the xy plane. Each histogram was an average collected over 5000 steps. They can be integrated into the density profiles (dN/dz) shown in Fig. 1. The system, which has a density higher than the triple point density, was originally in the liquid state $T^* \equiv k_B T/\epsilon = 3.38$, see Fig. 2(a). It was then quenched to $T^* = 1.27$ [Fig. 2(b)], staying in a long-lived amorphous state for 35τ, before any nucleation could take place. The strong wall-fluid interaction $\epsilon_{wf} = 3.9\epsilon$ leads to significant anisotropy in the molecular orientations in the surface layers, favoring molecules inclined to the walls, with larger θ. (The accompanying increase in the number of surface molecules

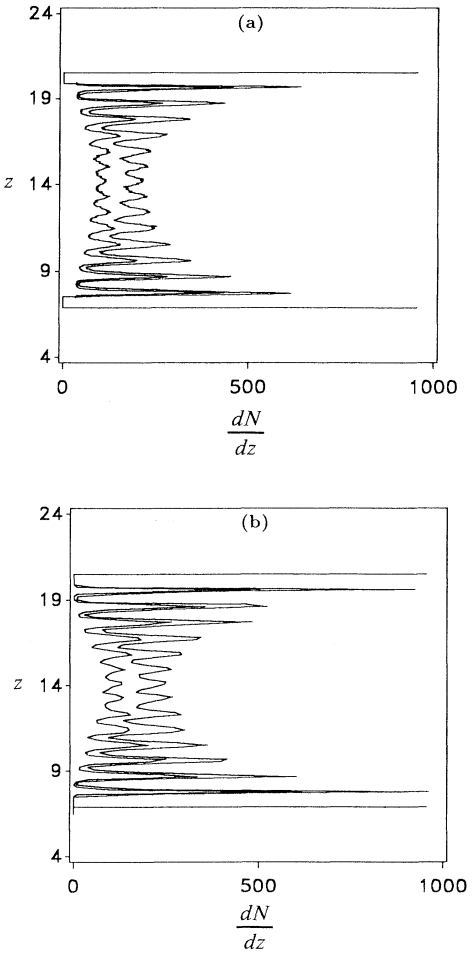

FIG. 1. The profile of dN/dz for system B with $\epsilon_{wf} = 3.9\epsilon_{ff}$, in units of σ^{-1}. The left curve corresponds to the molecular centers, whereas the right curve represents the atomic centers. The horizontal lines at the top and the bottom of the profiles denote the locations of the wall surfaces. (a) $T^* = 3.38$. (b) $T^* = 1.27$.

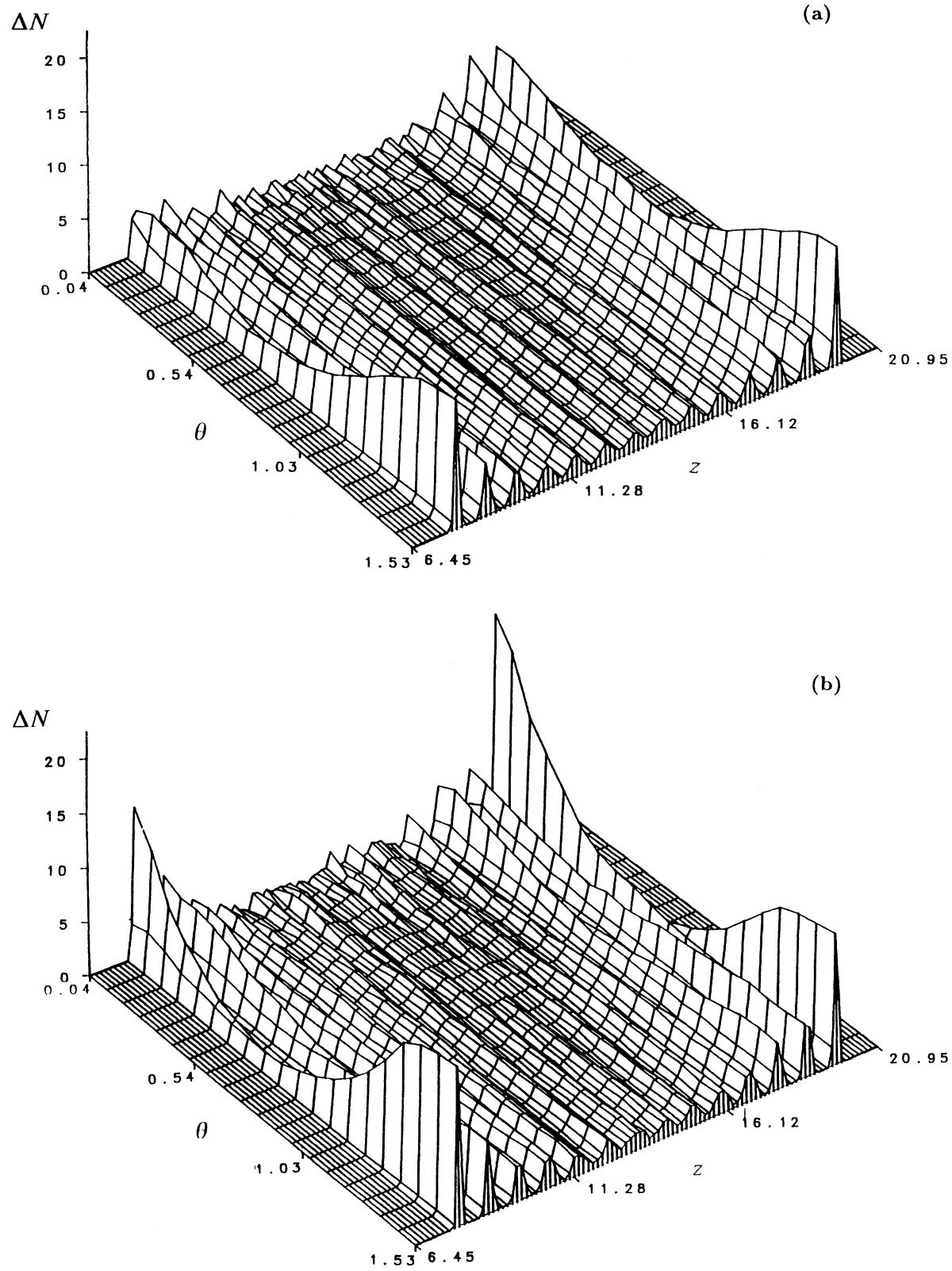

FIG. 2. The histograms of $\Delta N \equiv (d^2N/id\Omega dz)\Delta\theta\Delta z$ of the confined fluids, where $\Delta\theta$ and Δz are the bin sizes. We have 20 bins for θ, from 0 to $\pi/2$, and 100 bins over the gap in the z direction. (a) and (b): system B, same as (a) and (b) in Fig. 1, respectively.

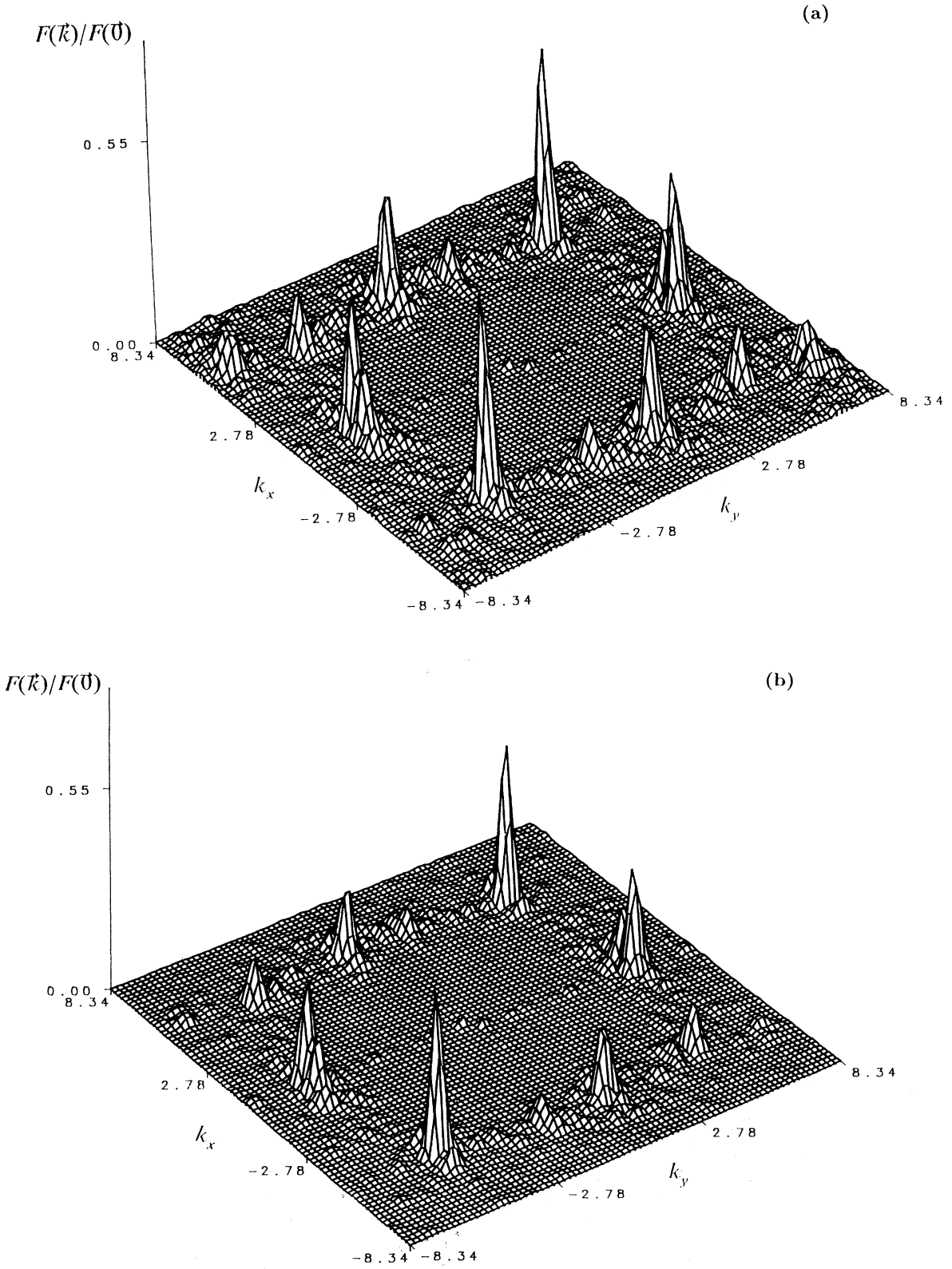

FIG. 3. The 2D structure factors of molecular centers (a) and atomic sites (b) in a surface layer of the frozen state described in Fig. 1(b). They have been normalized according to the peak value at $\mathbf{k}=(0,0)$. The broadened peak (due to finite size effects) at $\mathbf{k}=(0,0)$ in each plot has been removed by subtracting off $|4\sin(k_xL_x/2)\sin(k_yL_y/2)/k_xk_yL_xL_y|^2$, where L_x and L_y are the linear dimensions of the system in the x and y directions, respectively. (For a two-dimensional uniform random configuration, this works very effectively. On the other hand, its effect on the structure factor in the region of k space that we are interested in is negligible.)

nearly perpendicular to the walls, i.e., $\theta \sim 0$, is due to the preference of the T-shaped configurations for linear molecules [10,11].) This orientational preference, however, can hardly be seen in the region beyond the surface layers. Further analysis was carried out employing the 2D structure factors

$$F(\mathbf{k}) \equiv \frac{1}{N} \left| \sum_j e^{i\mathbf{k}\cdot\mathbf{r}_j} \right|^2 , \tag{2}$$

of a surface layer, for the molecule centers and for the interaction (atomic) sites (denoted by $F_c(\mathbf{k})$ and $F_a(\mathbf{k})$, respectively), see Fig. 3. The summation goes over the molecules or interaction sites. (Note that the broadened peak at $\mathbf{k}=(0,0)$ in each plot has been removed for clarity.) In Fig. 3, F_a is very similar to F_c, except that the sizes of the peaks are reduced. The lack of additional peaks in F_a, as compared with those in F_c, indicates that the in-plane bond orientations have very poor spatial correlations. Further evidence is obtained from the calculations of the ratio $F_a(\mathbf{k})/F_c(\mathbf{k})$ at their maximal peaks in the first Brillouin zone. If the configuration has a random and isotropic orientation distribution with molecules constrained parallel to the x-y plane, we expect

$$F_a(\mathbf{k}) \sim F_c(\mathbf{k}) \left| \frac{\sin(kl/2)}{kl/2} \right|^2 . \tag{3}$$

On the other hand, a random distribution isotropic in three dimensions leads to

$$F_a(\mathbf{k}) \sim F_c(\mathbf{k}) \left| \int_0^{\pi/2} \frac{\sin(kl\sin\theta/2)}{kl/2} d\theta \right|^2 . \tag{4}$$

Our result: $F_a(\mathbf{k}):F_c(\mathbf{k})=1.6:1$, is quite different from the predicted value ~ 1.0 of Eq. (3) and is close to 1.48, as predicted by Eq. (4). Indeed, the same calculations carried out for the bins in the center of the channel agree with Eq. (4). In Figs. 1(a) and 1(b), the locations of the peaks and troughs in the density profiles of the molecular centers coincide with those in the profile of the atomic sites. Furthermore, the ratio between the two profiles is very close to 2:1 in the region away from the surface, indicating a uniform distribution in the angle θ.

The quantitative analysis has also been applied to system A, where the density is below the triple point density. As expected, a surface layer in the static fluid is again characterized by weak translational ordering with the molecular axes oriented randomly in nearly all directions. In the presence of steady flows, it is interesting to see how the surface layers responds to the shear created by the moving fluid. We have studied the behavior of the molecules at the boundaries of a Poiseuille flow and a Couette flow (see Sec. III C). While the flow preserves the sharp oscillations in the density profile near a wall in each case, there is no evidence of induced translational ordering or orientational correlation either in the body of the flow [15] or within the surface layers in our simulations.

The weak translational ordering and the lack of orientational correlation in a surface layer has a far-reaching effect on the mechanism of freezing in system B. The surface layer behaves effectively as a rough surface with corrugations on a scale similar to the bond length of the dumbbell molecules as viewed by the other dumbbell molecules in the channel. The irregular corrugation reduces the preference for forming new layers on top of the surface layers. The induced layer-by-layer mechanism found in the spherical molecule fluid case [5], therefore, can only exist when such corrugations are negligible. We will come back to this in the next section. In the case of channel flows, previous studies [3,16] indicate, with proper macroscopic interpretation of the conditions at the boundaries, that the continuum description is good for the flow of fluid comprised of spherical molecules in a channel as narrow as ten molecular sizes. Since the randomly oriented surface molecules lose the ability to transmit ordering to the interior regions, it is important to find out whether the same description is valid in a narrow channel filled with a dumbbell fluid. This is the issue we are going to address in Sec. III C. Finally, in Sec. III D, we will check the effect of the orientational degrees of freedom on the stick-slip mechanism of two plates separated by a monolayer of dumbbell molecules.

B. Freezing

In the classical theory of homogeneous nucleation [17], a nucleus in an undercooled bulk liquid can grow into a crystallite only if its size is larger than a critical value. The nucleus undergoes a "catastrophic" growth due to the fact that an increase in its size lowers the free energy of the system. The picture has been extended to explain the observed dependence of transition temperature on the pore size, in a geometrically confined liquid [1]. In a MD study [5] of a quenched dense spherical molecule liquid confined in a channel, two possible candidate mechanisms were found. One is homogeneous nucleation, where the liquid in the channel solidifies simultaneously into a layered structure. The other mechanism entails freezing from the walls into the channel, in a layer-by-layer manner. The condition that determines which mechanism dominates is related to whether a solidlike surface layer already exists before quenching [5]. For a confined dumbbell molecule liquid, additional factors are introduced. The presence of orientational degrees of freedom weakens the ability of the surface layers to induce subsequent layers. The layer-by-layer mechanism will dominate only when the corrugation arising from the orientational degrees of freedom is negligible. To verify these ideas, in addition to system B, we have carried out MD simulations on a system (system D in Table I) of dumbbell molecules with a tiny bond-length $l=0.1085\sigma$, confined in a channel of the same size as in system B. While there

TABLE I. Summary of systems considered in this study.

System	ρ^*	gap/σ	l/σ
A	0.63	16.82	0.329
B	0.836	12.85	0.329
C	0.93	1.9	0.329
C_1	0.93	1.9	0.0
D	0.836	12.85	0.1085

is no evidence of layer-by-layer nucleation in system B, we found that this mechanism prevails in system D, which has the same density as in system B. We present more details below.

System D with wall-fluid interaction strength $\epsilon_{wf}=3.9\epsilon$ was quenched instantaneously to $T^*=0.9\epsilon$ in the first stage, followed by an ultimate increase to $T^*\sim 1.27\epsilon$ in the next two stages. At each stage, we let the system evolve isothermally for 5τ, followed by an equal amount of time of adiabatic evolution. We found that the layer-by-layer nucleation proceeded steadily, in spite of the temperature variations. Figure 4(a) shows the snapshot at $t=20\tau$ following the first quenching. We see two sharp layers near the wall. In Fig. 4(b), at $t=30\tau$, there are 14 well-defined layers filling the whole channel. While the peak values of the normalized 2D structure factors (Debye-Waller factors) of the surface layers have saturated, those for the second layers near the two walls increases by a factor of ~ 1.5 during the interval between $t=20\tau$ and 30τ. These feature are quite consistent with those of the layer-by-layer freezing mechanism found in the quenched dense spherical molecule fluid. Note that, since the triple point shifts towards the higher density and higher temperature region in the phase diagram on reducing the bond length, the density of system D is quite close to the triple point density (~ 0.80 [18]). Thus this mechanism should prevail at higher densities, where the close-packing effect is enhanced. As mentioned in Sec. III A, system B does not display this mechanism under similar conditions.

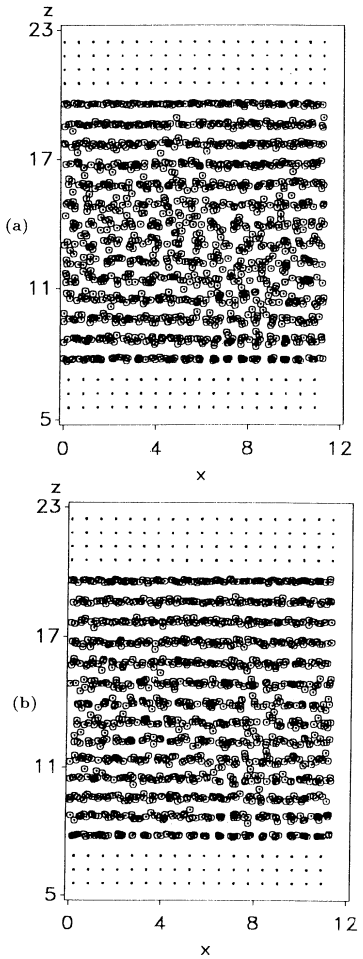

FIG. 4. The projection of snapshots of system D on the x-z plane, with $\epsilon_{wf}=0.7\epsilon$. (a) $t=20\tau$ and (b) $t=30\tau$. The quenching started at $t=0$.

In order to determine the properties characterizing the two competing mechanisms, we have also prepared a quenched system which is governed by homogeneous nucleation. We choose system B, with wall-fluid interaction strength $\epsilon_{wf}=0.7\epsilon$ as our sample system. We found a strong structure arrest in system B that prevented the system from relaxing into a more ordered state within the time scale of our simulations. Instead of preparing the frozen state directly, we started with the final ordered configuration of system D and changed the bond length and the wall-fluid interaction to the desired values. We then tested the stability of the new system (system B now), after relaxation, against a heat pulse followed by adiabatic relaxation. We found that the partially-ordered state with layered structure was stable within the time we probed (40τ).

We have checked the microscopic molecular dynamics of the two systems by calculating the autocorrelation functions of the molecule center of mass velocity $C_v(t)=\langle \mathbf{v}(t)\cdot\mathbf{v}(0)\rangle$ and of the molecular orientation $C(t)\sim\langle \mathbf{b}(t)\cdot\mathbf{b}(0)\rangle=\langle\cos\theta(t)\rangle$, where $\mathbf{b}(t)$ is the unit vector along the bond of a dumbbell molecule at time t. The averages were taken over both the initial time and over the different molecules. In order to characterize the z dependence of these correlation functions, the channel of each system was divided into two surface regions, each consisting of the layer of surface molecules near a wall, and three central regions which equally partitioned the rest of the channel. In the simulations, whenever a molecule leaves one region, its contribution to the old region is terminated and that to the new region is initiated simultaneously. Whenever there is no detectable differences among the correlation functions over the three central regions, we combined the three regions into one single region. Figures 5(a) and 5(b) show the velocity autocorrelation functions for system B and system D, respectively. While there is no spatial dependence of the translational motion in the region beyond surface layers in system B, such dependence does exist in system D. The spatial dependence, on the other hand, does not exist for the molecular orientational degrees of freedom in both systems (see Fig. 6). The fast decays in the molecular orientation autocorrelation function of system D [Fig. 6(b)], however, indicate the molecules are less hindered in rotation than those in system B [Fig. 6(a)]. We conclude that a system subject to layer-by-layer freezing mechanism is characterized by stronger spatial heterogeneity in its molecular translation motion [5].

C. Steady flows

In the previous MD studies of steady flows confined by molecular walls, the spherical molecule fluids displayed behavior consistent with continuum hydrodynamics in channels as narrow as ten molecular sizes [3,5,16]. The

microscopically evaluated profiles of momentum flow and velocity, agree very well with the predictions by the continuum equations, if a properly chosen microscopic length is used to quantify the location of an interface at a boundary. This length was found to be closely related to the in-plane ordering of the layer [5]. While the surface layers of a confined dumbbell molecule fluid are characterized by more complicated properties, it is sensible to ask the question whether the phenomenological description applies to the flows.

We generated flows in system A, which was in contact with that thermal bath at temperature $T^*=3.23$. A Poiseuille flow as obtained after applying a constant acceleration $g=0.086\sigma\tau^{-2}$ to each site of the dumbbell molecules in the x direction for 140τ. Couette flow was established after translating the walls at $\pm 1.1952\sigma\tau^{-1}$ for 100τ. On tuning the strengths of the wall-fluid interactions, we produce flows with two different boundary conditions for each type of flow. They are identified as slip and no-slip boundaries, respectively.

At the continuum level, one expects that for Poiseuille flow, the velocity profile, and the stress tensor are given by [19]

$$u^x=\frac{p'}{2\eta}(z-z_1)(z_2-z) \tag{5}$$

and

$$\pi^{xz}=p'(z-z_c)\ , \tag{6}$$

respectively, where z_1, z_2, and $z_c\equiv\frac{1}{2}(z_1+z_2)$ are the locations of the two boundaries and the center of the channel. $p'\equiv\partial p/\partial x$ is the pressure gradient along the x direction. For Couette flow, the corresponding equations [19] are

$$u^x=\frac{2u_0}{h}(z_c-z) \tag{7}$$

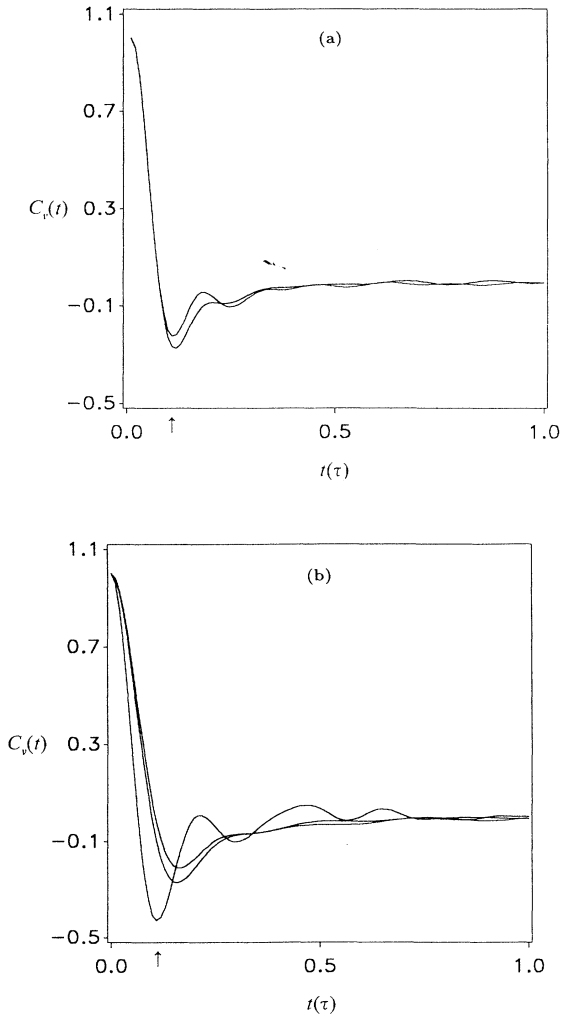

FIG. 5. The center-of-mass velocity autocorrelation functions (a) of system B in its amorphous frozen state (at the time indicated by the arrow: lower, surface layer; upper, central region). (b) System D in its frozen state (from bottom to top at the time indicated by arrow, the surface layer, intermediate region, and the central region).

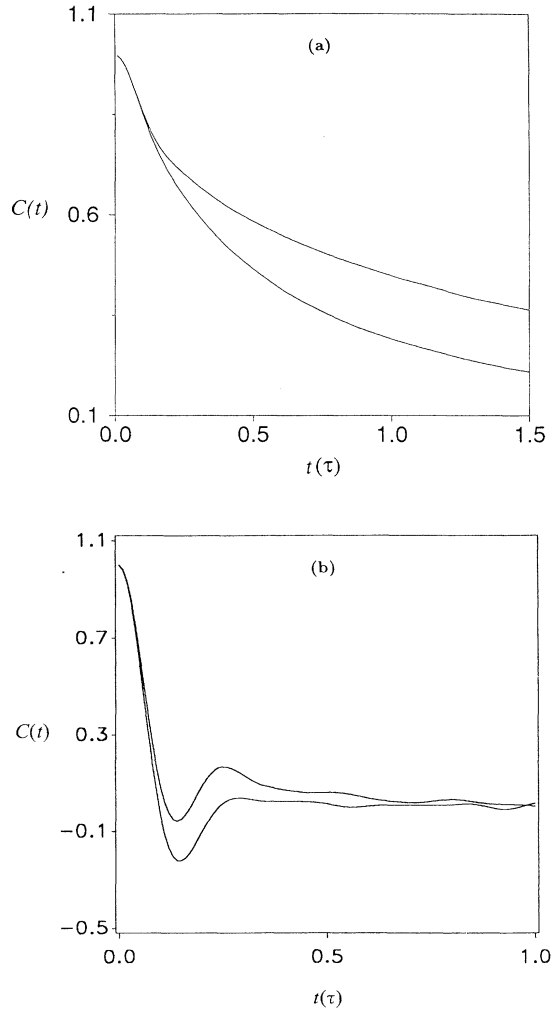

FIG. 6. Plots of the bond-orientation autocorrelation functions of system B (a) and D (b) in their frozen states. (Upper, surface layer; lower, central region.)

and

$$\pi^{xz}=\frac{2u_0\eta}{h} \tag{8}$$

with the gap size $h\equiv|z_1-z_2|$ and the relative speed $2u_0$ between two walls. In our calculations [20], we chose the size and locations of the bins matching the surface layers. The data were collected as averages over 20 000 steps in each case. Figures 7(a) and 7(b) show the profiles of velocity and stress tensor for steady Poiseuille flows with two different wall-fluid interaction strengths. Taking η, z_1, z_2, and p' as fitting parameters [Eqs. (5) and (6)], we found that the profiles of the velocity and the stress tensor fit nicely to parabolic curves and straight lines, respectively. We get estimates of the shear viscosity η, and the slip length δ which is defined as the difference between the phenomenological boundaries (z_1,z_2) and the physical boundaries (the locations of the surface bins). We found that the δ for the case with wall-fluid interaction strength $\epsilon_{wf}=5.571\epsilon_{ff}$, is less than one quarter of the width of a bin. In the other case, where $\epsilon_{wf}=3.286\epsilon_{ff}$, δ is close to the size of a bin. We regard the two cases as no-slip and slip at boundaries, respectively. The estimated shear viscosities are 3.84 and 3.22 (in reduced units $m\sigma^{-1}\tau^{-1}$, where $m\equiv M/2$), respectively. In the case of Couette flow, we also have no-slip and slip boundaries, see Figs. 7(c) and 7(d). The viscosities determined by the relation $\eta=\pi^{xz}/(\partial u^x/\partial z)$, are $\eta\sim3.35$ and 3.81, respectively. These values of η agree with each other within the error bars [21,22].

From the calculation of the 2D structure factor [Eq. (2)] of the molecular centers, we see a decreasing of ordering from no-slip to slip at boundaries in both the Poiseuille and Couette flows. This agrees with the results from simulations of spherical molecules [6]. An analysis of the molecular orientation correlation functions of molecules has also been applied to the flows. While the behavior of molecules in surface layers are dependent on

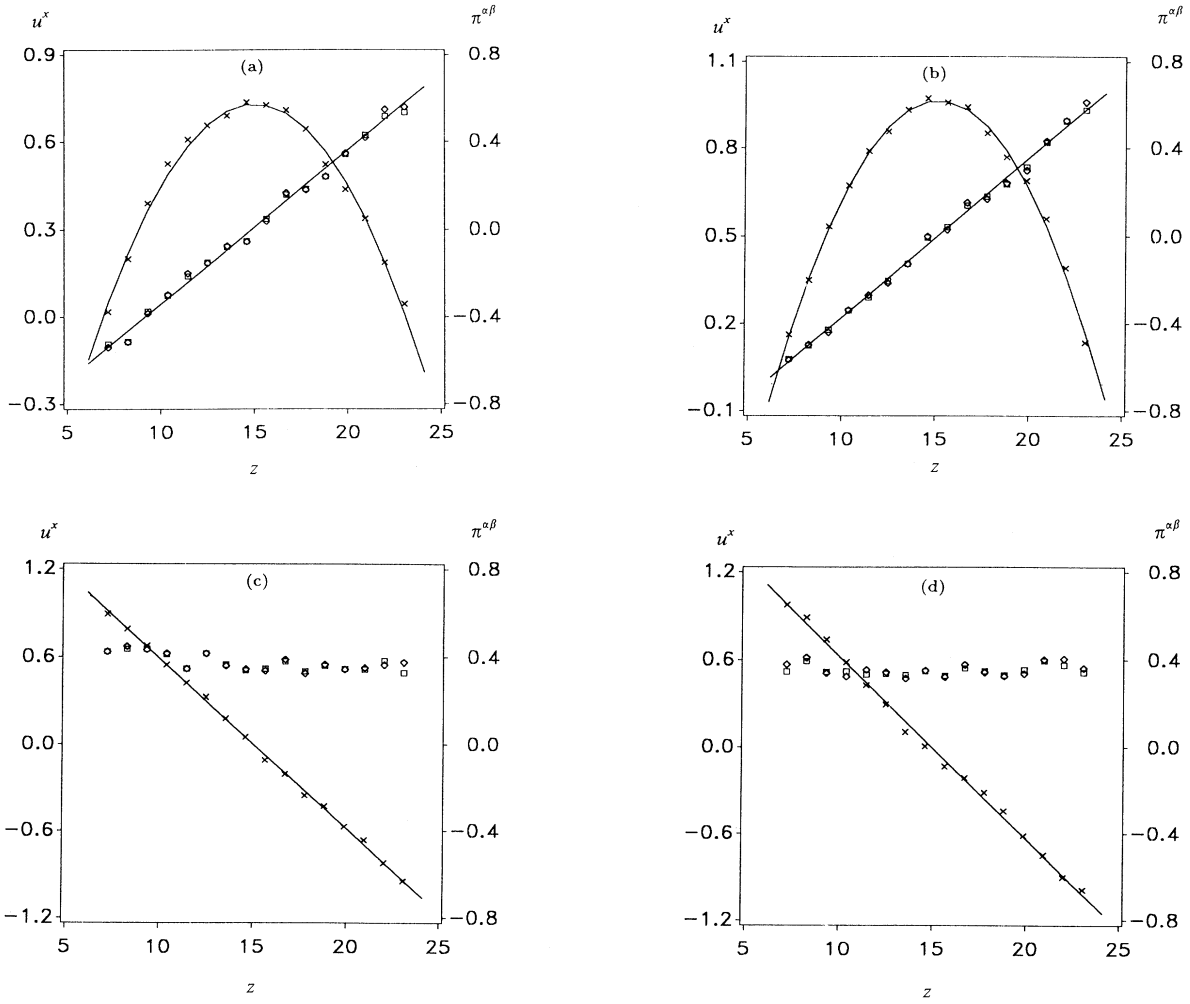

FIG. 7. The profiles of velocity u^x (cross, left vertical coordinate) and off diagonal stress tensors π^{xz} (square) and π^{zx} (diamond, right vertical coordinate), for steady Poiseuille flows (a) and (b), and Couette flows (c) and (d). The wall-fluid interaction strengths are $\epsilon_{wf}=5.571\epsilon_{ff}$ for (a) and (c) and $\epsilon_{wf}=3.286\epsilon_{ff}$ for (b) and (d). The labeled values on the vertical axes should be multiplied by 1.1952 to get the correct value in the reduced units.

the wall-fluid interactions, the reorientational dynamics of molecules in the rest of the channel, has no dependence on either the global pattern of the flows or on the boundary conditions.

D. Stick-slip friction

In the narrow channel of system C, the lubricant layer is still characterized by imperfect translational ordering as a result of the orientational degrees of freedom. This is true even for a system of monolayer dumbbell molecules. As shown in the preceding two sections, a study of the dynamical features can lead to more insight about the nature of the phenomenon. For this purpose, we have also carried out simulations for spherical molecules (system C_1). Monolayer lubricant molecules were employed in both systems to facilitate detailed analysis of the configurations. The systems were attached to a thermal bath (see Sec. II). The two plates are held together by opposing constant force fields, of magnitude $17.5m\sigma/\tau^2$, on the wall atoms of the cubic cells not in contact with the fluid. The same layers of walls acted as a thermal bath as described above. Thus our system is effectively in a constant load environment. The stick-slip motion was produced by a spring, with spring constant $5.0m/\tau^2$, dragging the upper plate with a speed $0.05\sigma/\tau$, in the x direction, relative to the static lower plate.

In Fig. 8, we show the time evolution of the spring force, the gap size, the effective temperature, and the 2D Debye-Waller factor [see Eq. (2)], for system C_1. The thermal bath was at a temperature $T^*=1.1$. Due to the periodic atomic corrugations on the wall surfaces, there were two selected directions for the orderings. They are along $k_x=\pm k_y$. The data shown for the Debye-Waller factor in Fig. 8 were therefore selected in the vicinity of these two directions. As can be seen in Fig. 8, the slip motion is characterized by the dropping in the peak values of the structure factor, accompanied by the release of heat and the expansion of the gap [7]. The short lifetime of the disordered "slip" state, as compared with the previous studies [7], is due to the effectively higher density in our lubricant layer (we have a monolayer of 112 molecules, which is approximately the number of molecules sitting on a surface layer in a liquid confined in a wide channel of reduced density $\rho^*\sim 0.93$). Since the plates have finite masses (the total mass of each wall is ~ 15 times of the total mass of the lubricant film), the top plate underwent small amplitude oscillations in the x direction during the "stick" periods, as a result of the combined effect of the elastic couplings provided by the lubricant layer between the two plates, and the spring force from the external spring. With an increased spring force, the oscillations persist with a decaying amplitude [Fig. 8(a)], due to the stiffer coupling between the two plates [23]. Note that when the system starts to slip, the heat release and the gap expansion occur slightly after the initiation of the slip motion [Figs. 8(b) and 8(c)]. This suggests that they originate from the transfer of kinetic energy from the wall molecules to the lubricant layer. We have carried out detail examinations of the snapshots of the evolving system. We found that the mechanism in this simple system can be characterized by a selection process induced by the increasing stress. In the "stick" state, at any given stress one may study the distribution of states that the lubricant molecules explore. As the spring force increases, we find that this distribution becomes narrower corresponding to a selection among these states. The increased stress favors configurations which lead to a stronger coupling between the plates. In these configurations, the relative position of the two plates allows an increase in the number of wall atoms in contact with each lubricant molecule (i.e., there is a high "bond number" between the lubricant molecules and the wall atoms), in this monolayer case, see Fig. 9. This tendency is also characterized by decreasing fluctuations in the variations in the gap size, the effective temperature and the Debye-Waller factor [Figs. 8(b) and 8(d)].

With dumbbell molecules as the lubricant layer, the stick-slip motion basically retains most of the features that appeared in the system with spherical molecules, see Fig. 10. The are two major differences. In the stick state, the translational ordering is not necessarily high all the time [see Fig. 10(d)], as a result of the effect of the rotational degrees of freedom in a direction perpendicular to the plane of the film. The high translational ordering appears only near the end of the stick state, when the high stress selects out these "stiffest" configurations. A de-

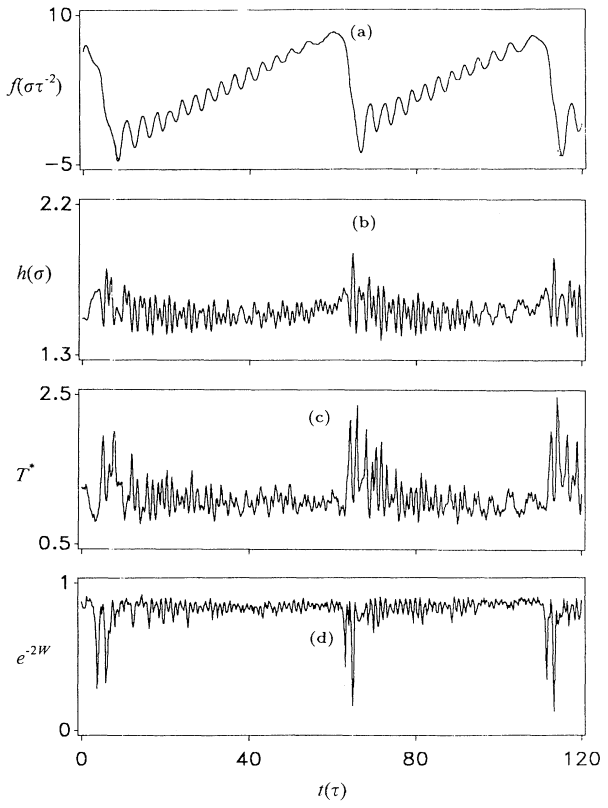

FIG. 8. The (a) spring force, (b) gap size, (c) effective temperature, and (d) 2D structure factor of the molecular centers, as functions of time in the stick-slip motion in system C_1 comprised of spherical molecules.

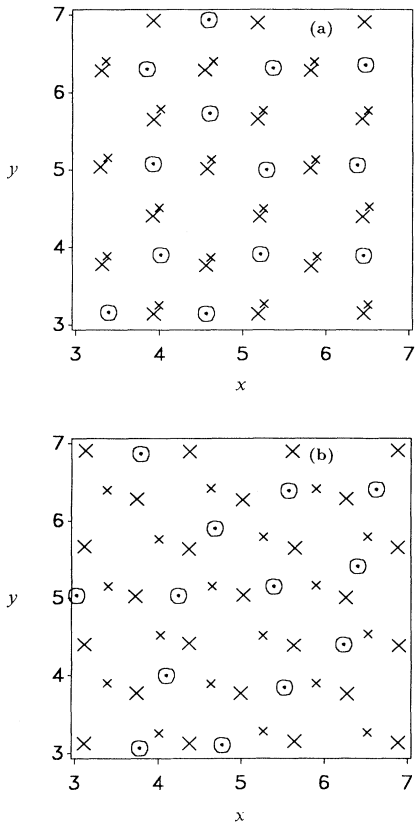

FIG. 9. Section of the snapshot (a) at $t=85\tau$ and (b) at $t=110\tau$. [We show only the wall atoms on the surfaces of the top (large cross) and the bottom (small cross) walls, respectively. The circles correspond to the lubricant molecules.]

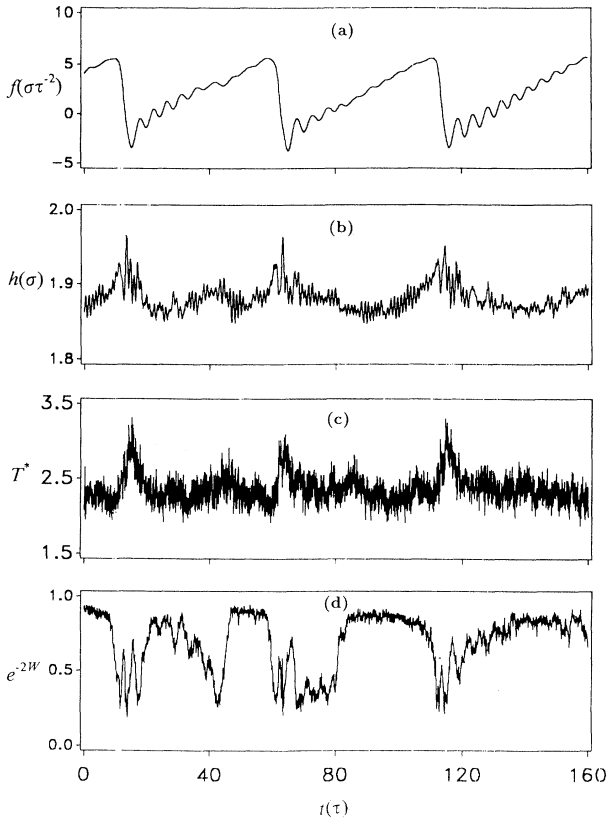

FIG. 10. The (a) spring force, (b) gap size, (c) effective temperature, and (d) 2D structure factor of the molecular centers, as functions of time in the stick-slip motion in system C comprised of dumbbell molecules.

tailed check of the snapshots shows that collective behavior more complex than the simple bond-number criterion dominates the mechanism. As a result, the second major difference between the spherical molecule lubricant layer and the dumbbell molecule case is the irregular fluctuations in the gap size and the effective temperature during the "stick" state in the latter case [Figs. 8(b) and 8(c)], in contrast to the decreasing fluctuations in the former case. Nevertheless, the high translational ordering is still characteristic of the stiffest configurations. In summary, the state of the lubricant in the stick state is characterized by a continuing decrease in the entropy induced by the increasing tangential stress [24]. When the stress exceeds the maximum endurable by the lubricant, the system yields to the slip motion.

IV. SUMMARY

The existence of surface layers in geometrically confined simple liquids [14,25] results from a close-packing effect. For spherical molecule fluids in the presence of flat walls, sharp oscillations in the density profile, in the regions near the walls, are observed. Solidlike surface layers with in-plane 2D translation ordering are present due to the (attractive part of the) wall-fluid interactions [5,6]. MD studies show that this ordering is directly related to boundary-layer properties [6], the state of lubricant in stick-slip motion [7], and the ability to induce nucleation [5]. For systems made up of dumbbell molecules, while there is well-defined perpendicular ordering near the walls, the interplay between the translational and orientational degrees of freedom weakens the in-plane ordering. The significance of this effect on the 2D ordering is determined by the bond-length-to-molecule-size ratio [26]. A poor in-plane ordering of the surface layers make them look like "rough" surfaces to the rest of the dumbbell molecules. The nearly randomly oriented molecules on the surface layers effectively "soften" the potential felt by the molecules inside the channel. Thus, the reorientation dynamics of the molecules other than in the surface layers, is the same as their counterpart in the compressed system without confining walls. Even though the density layering is found in the interior of the channel, the transverse spatial correlations characterizing the wall surfaces are not significantly transmitted into the channel. In steady flows, the boundary layers are typically "thinner" than in the case of spherical molecular flows. For the quenched dense liquids, the closed-packed layered structure can be reached via either the layer-by-layer freezing mechanism or a homogeneous nucleation, depending on the length of the molecules.

In the experimental studies of freezing in porous glasses [1], the orientational relaxation of confined quenched liquids, have two characteristic time parameters as compared with only one parameter in the relaxation of bulk liquids. Our simulation of confined systems show reorientations characterized by many time scales. These arise from the same group of molecules in contrast to the situation in the experiments, where there are two separate processes involving the confining bulk and the surface layers, respectively. Since, for both a liquid in the central region of the confined system and a "bulk" liquid subject to periodic boundary conditions at the same temperature and density, the orientational correlations are virtually identical, the same dynamics governs the compressed metastable state in the two cases. The qualitative difference between the reorientation dynamics of our "bulk" system and that of the bulk system considered in the experiment, even in their liquid states, suggests that a more complex dynamics is involved in the compressed state. On the other hand, the effects of the irregular geometry in the porous glass and the more complicated wall-fluid interactions that could break the symmetry between the two interaction sites on the dumbbell molecules, were not included in our simulations. These effects may lead to new configurations for the surface region, which would then result in different reorientational dynamics characterizing the surface layers. A similar effect may also lead to the interplay between the wall-induced freezing and the homogeneous nucleation leading to the variety of structures observed in the experiment [4].

The systems that we have considered in our stick-slip mechanism have only a monolayer of lubricant molecules. With plates of light mass, the system generates several signatures which facilitated a detailed analysis of the origin of the mechanism. The conclusions are quite readily extended to systems with thicker layers. The important feature in a film with multimolecular layers is the better-defined (thermodynamic) solid and liquid states, due to the possibility of coherence in the direction perpendicular to the plate surfaces. The stick-to-slip mechanism would then be a phase transition between the stressed solid state and the liquid states [7].

We are indebted to Mark Robbins, Paul Sokol, and Bill Steele for stimulating discussions. We gratefully acknowledge that the financial support provided by NSF and NASA and grants of computer time by the Pittsburgh Supercomputer Center, the Center for Academic Computing of The Pennsylvania State University, and the SERC at the Indian Institute of Science. LKI thanks the UGC (Government of India) for support. JRB is grateful to USAID for support under the Indo-U.S. Science and Technology Fellowship Program.

[1] D. D. Awschalom and M. W. Schafer, Phys. Rev. Lett. **57**, 1753 (1986); *Molecular Dynamics in Restricted Geometries,* edited by J. Klafter and J. M. Drake (Wiley, New York, 1989).

[2] J. N. Israelachvili, P. M. McGuiggan, and A. M. Homola, Science **240**, 189 (1988); M. L. Gee, P. M. McGuiggan, J. N. Israelachvili, and A. M. Homola, J. Chem. Phys. **93**, 1895 (1990).

[3] J. Koplik, J. R. Banavar, and J. F. Willemsen, Phys. Fluids A **781**, (1989); M. Sun and C. Ebner, Phys. Rev. Lett. **69**, 3491 (1992).

[4] P. E. Sokol, W. J. Ma, K. W. Herwig, W. M. Snow, Y. Wang, J. Koplik, and J. R. Banavar, Appl. Phys. Lett. **61**, 777 (1992); P. E. Sokol (unpublished).

[5] W. J. Ma, J. R. Banavar, and J. Koplik, J. Chem. Phys. **97**, 485 (1992).

[6] P. A. Thompson and M. O. Robbins, Phys. Rev. A **41**, 6830 (1990).

[7] P. A. Thompson and M. O. Robbins, Science **250**, 792 (1990); M. Lupkowski and F. van Swol, J. Chem. Phys. **95**, 1995 (1991).

[8] H.-W. Hu, G. A. Carson, and S. Granick, Phys. Rev. Lett. **66**, 2758 (1991); P. A. Thompson, G. S. Grest, and M. O. Robbins, *ibid.* **68**, 3448 (1992).

[9] J. N. Glosli and G. M. McClelland, Phys. Rev. Lett. **70**, 1960 (1993); M. W. Ribarsky and U. Landman, J. Chem. Phys. **97**, 1937 (1992).

[10] P.S.Y. Cheung and J. G. Powles, Mol. Phys. **30**, 921 (1975); M. Wojcik, K. E. Gubbins, and J. G. Powles, *ibid.* **45**, 1209 (1982).

[11] J. P. Hansen and I. R. McDonald, *Theory of Simple Liquids,* 2nd ed. (Academic, London, 1986).

[12] M. P. Allen and D. J. Tildesley, *Computer Simulation of Liquids* (Claredon, Oxford, 1987).

[13] See, e.g., R. D. Diehl, M. F. Toney, and S. C. Fain, Phys. Rev. Lett. **48**, 177 (1982); A. D. Migone, H. K. Kim, M. H. W. Chan, J. Talbot, D. J. Tildesley, and W. A. Steele, *ibid.* **51**, 192 (1983); S. Sokolowski, Mol. Phys. **75**, 999 (1992).

[14] J. Magda, M. Tirrell, and H. T. Davis, J. Chem. Phys. **83**, 1888 (1985); M. Shoen, J. H. Cushman, D. Diestler, and C. L. Ryhkerd, *ibid.* **88**, 1394 (1988); S. Toxvaerd, *ibid.* **74**, 1998 (1981).

[15] W. Xue and G. S. Grest, Phys. Rev. **64**, 419 (1990); M. J. Stevens and M. O. Robbins, Phys. Rev. E **48**, 3778 (1993).

[16] L. Boiquet and J.-L. Barrat, Phys. Rev. Lett. **70**, 2726 (1993).

[17] F. F. Abraham, *Homogeneous Nucleation Theory* (Academic, New York, 1974).

[18] D. B. McGuiggan, M. Lupkowski, D. M. Paqeut, and P. A. Monson, Mol. Phys. **67**, 33 (1989).

[19] L. D. Landau and E. M. Lifshitz, *Fluid Mechanics* (Pergamon, Oxford, 1987).

[20] The microscopic expression for the components of the stress tensor, evaluated in a bin at position z, is

$$\pi^{\alpha\beta}\equiv\left\langle\frac{1}{\delta w}\left[\frac{1}{2}\sum_{i\in z}\sum_{j}f_{ij}^{\alpha}r_{ij}^{\beta}+M\sum_{i\in z}v_i^{\alpha}(v_i^{\beta}-u^{\beta})\right]\right\rangle,$$

where molecule j, either belonging to the walls or the fluid, exerts a force $\mathbf{f}_{ij}$ on molecule i, at a relative position $\mathbf{r}_{ij}=\mathbf{r}_i-\mathbf{r}_j$. δw and $\mathbf{u}$ are the volume and the average ve-

locity in the bin, respectively. $\mathbf{v}_i$ is the velocity of molecule i. [See Ref. [11] or J.H. Irving and J. G. Kirkwood, J. Chem. Phys. **18**, 817 (1950).]

[21] We calculated the error bars of the shear viscosity η by considering the deviations in the simulation data from their fitted curves. The data for the Poiseuille flow shown in Fig. 7(a), have 9% and 11% error bars in the fitting parameters when they are fitted according to Eqs. (5) and (6), respectively. They account for a total error estimate of 20% for η. The same estimation of the error bars for Fig. 7(b) are 3% and 12%, respectively, which accumulate to 15%. [Note that the momentum flux pumped by the external acceleration g would lead to a pressure gradient $p'=\rho g$ in the x direction. We found that the p' fitted from Eq. (6) is systematically less than ρg. This is because the contributions of the external x-momentum flux in the x direction from the walls are not negligible in a narrow channel.] Based on a similar analysis, there are 16% and 13% error bars for the two Couette flow cases, shown in Figs. 7(c) and 7(d), respectively.

[22] The condition in our simulations is equivalent to nitrogen at a temperature $T=120$ K and the diagonal elements $\pi^{xx}\sim\pi^{yy}\sim 1340$ bar. (For nitrogen, $\sigma=3.31$ Å and $\epsilon=37.3k_B$.) On the experimental side, at temperature 120 K and pressure 500 bar, the viscosity is 110.8×10^{-6} N s m^{-2}, which is equal to $3.46m\sigma^{-1}\tau^{-1}$. See, e.g., K. Stephan and K. Lucas, *Viscosity of Dense Fluids* (Plenum, New York, 1979).

[23] On the macroscopic level, the top plate has a conserved total mechanical energy. As the elastic coupling between the two plates increases, so does the overall spring constant, which leads to a decrease in the amplitude.

[24] As the probability distribution becomes narrower, the entropy becomes smaller. Consider a two-state system. The entropy S of the system can be written as $S/k_B=-p_1\ln(p_1)-p_2\ln(p_2)$, where p_i is the probability of state i ($p_1+p_2=1$.) It is obvious that a uniform distribution has a larger entropy than that of a distribution with $p_i=1$. The general case can be proved by a similar argument leading to the Gibbs-Bogoliubov inequality (p. 152 of Ref. [11]).

[25] In the equilibrium liquid case, it has been shown that [J. Fischer and M. Methfessel, Phys. Rev. A **22**, 2836 (1980)] using the pair correlation functions as input, that the solutions of the Born-Green-Yvon hierarchical equations (see Ref. [11] for a detailed discussion of these equations) lead to oscillations in density profiles near a wall which agrees with the simulation data. It would be interesting to extend it to the steady flow case.

[26] For example, a naive estimation of the bond-length at which the surface layer loses its ability to have 2D structure for system B is as follows. We adapt the Lindeman rules of melting as our criteria of losing 2D ordering on the surface layer, i.e., when

$$F_a(\mathbf{G})/F_a(0)\sim[F_c(\mathbf{G})/F_c(0)]\left|\int_0^{\pi/2}\frac{\sin(Gl\cos\theta/2)}{(kl/2)}d\theta\right|^2 < 0.6$$

[the value is actually relevant for 3D structures, see M. J. Stevens and M. O. Robbins, J. Chem. Phys. **98**, 2319 (1993)], G is the shortest reciprocal vector length. We put $F_c(\mathbf{G})/F_c(0)\sim 0.72$, which is the datum from system D. The result $l_c\sim 0.255\sigma$ gives an upper bound for the bond length when the wall-induced nucleation dominates.